Contrib. Astron. Obs. Skalnaté Pleso **37**, 125 – 141, (2007)

Comparisons of the green-line corona brightness with the magnetic field strength and the summary sunspot area

O.G. Badalyan[1], **N.G. Bludova**[1] **and J. Sýkora**[2]

[1] *Pushkov Institute of Terrestrial Magnetism, Ionosphere and Radio Wave Propagation, 142190 Troitsk, Russia*

[2] *Astronomical Institute of the Slovak Academy of Sciences 059 60 Tatranská Lomnica, The Slovak Republic*

Received: October 25, 2006; Accepted: May 3, 2007

Abstract. Comparisons of the Fe XIV 530.3 nm coronal emission line brightness with the summary area of sunspots and the magnetic field strength (extrapolated from the photospheric measurements to the 1.1 $R_\odot$ distance in the corona), are discussed. Different correlations of the coronal green line brightness (CGLB) with the large-scale coronal magnetic fields and the local fields of sunspots are found during different solar cycle phases. At the ascending phase of activity the large-scale coronal magnetic fields dominate, whereas at the descending phase a somewhat higher correlation of the CGLB with the local magnetic fields of sunspots is observed. It is shown that within the $\pm 40^\circ$ solar low-latitude zone a portion of the CGLB originating due to the large scale magnetic field amounts to 25-30% in the period of solar cycle maximum but it goes up to 85% at the cycle minimum. Impact of the local sunspot fields on the CGLB level is remarkably lesser, it provides only 8-10% of the CGLB during cycle maximum and increases to about 18% at its minimum. Results of this paper could be helpful when testifying various models of the solar corona heating.

Key words: coronal green line brightness – area of sunspots – magnetic field strength – mutual and solar cycle relations

1. Introduction

Role of the magnetic field is decisive in different active processes on the Sun, it controls origin and determines a cyclic character of the Sun's activity. Under a direct magnetic field influence the heating of the solar corona is realized. Various structural features filled by a hot plasma occur in the solar corona. These structures radiate mostly in the EUV and X-ray ranges, and in the optical emission lines, as well. In order to disclose how the magnetic field influences

physical processes in the corona one should analyze relationships of the coronal radiation in different spectral ranges with the magnetic field parameters.

Any effort to estimate quantitative relations between different solar activity indices and the magnetic field parameters seems to be perspective in the said direction. The λ 530.3 nm Fe XIV CGLB belongs to the most informative indices in helping to fulfil the task. This line originates at the temperature of ~ 2 MK which is most favourable for the Fe XIV ion to be generated. The brightness of the 530.3 nm forbidden emission line characterizes the level of activity in the solar corona. It shines brightly namely inside dense equatorial loops of the inner corona. On the contrary, the CGLB is substantially reduced within the high-latitude tenuous and cold regions, closely resembling coronal holes (e.g., Fisher and Musman, 1975; Letfus *et al.*, 1980; Sýkora, 1992; Guhathakurta *et al.*, 1996). A specific advantage of the CGLB index results from its almost simultaneous registration at all helio-latitudes. This allows comparative studies of the CGLB both in the dense equatorial coronal regions and in the polar coronal holes type regions. Relations of the inner corona structures and the CGLB with the magnetic field topology and strength were studied, e.g., by Guhathakurta *et al.* (1993), Wang *et al.* (1997), Rušin and Rybanský (2002).

Presently, comparisons of the EUV and X-ray coronal radiations, as measured on the solar disk, with evolution of active regions are well possible because the relevant EUV and X-ray data taken with a relatively high space and time resolution are now accessible during more than one solar cycle. For example, Zhang *et al.* (1999) have studied relation of the 171 Å coronal line radiation with photospheric magnetograms.

Our work on quantitative estimations of the CGLB relationships with the magnetic fields of different scales started by Badalyan and Obridko (2004; 2006), Bludova (2005) and Bludova and Badalyan (2006).

Bludova (2005) has compared the CGLB with the areas and positions of sunspots (representing, in fact, the regions of concentrated local magnetic field emergence on the solar surface) for a number of chosen Carrington rotations. She revealed that during individual periods of time, particularly, close to the minima of 11-year cycles, a very good correspondence is observed between the CGLB and the sunspot activity indices. It was shown, however, that such a correspondence does not survive and it is heavily disturbed during the maxima of cycles.

Bludova and Badalyan (2006) performed a detailed comparison of the CGLB with the areas and positions of sunspots for the 1977-2001 period. Unlike Bludova (2005) the last comparison was made exploiting the synoptic charts averaged over six Carrington rotations. It has been noticed that the local fields of sunspots and the large-scale coronal fields are differently connected with the CGLB at different phases of the solar cycle.

Cross-correlations of the CGLB and magnetic field synoptic charts (i.e., correlation coefficients for the sets of spatially corresponding points on charts), both averaged over six successive Carrington rotations, were presented in Badalyan

and Obridko (2004; 2006). It was found that the corresponding correlation coefficients depend strongly on the solar latitude and the phase of activity cycle.

In this work, we continue to study the coupling between the green-line emission of the inner corona and magnetic fields of various scales over long time intervals. We are considering the relationship of the local sunspot fields and the large-scale coronal fields with the brightness of the 530.3 nm XIV line.

We confirm here the conclusions of Bludova and Badalyan (2006) stating complicated relations between the CGLB, on the one hand, and the local sunspot magnetic fields and the large-scale coronal magnetic fields, on the other hand. We provide also some quantitative estimations about the degree to which the sunspots and the large-scale coronal magnetic fields affect the structures and physical conditions in the corona which determine the character of radiation in the coronal 530.3 nm line.

2. Observational data and procedure used

In the process, the synoptic maps of the CGLB distribution were constructed by Badalyan *et al.* (2004; 2005) and the charts of the magnetic field strength were calculated by Badalyan and Obridko (2004) under a potential approximation for the distance of 1.1 $R_\odot$ from the Wilcox Solar Observatory photospheric measurements. The coordinates and areas of the sunspot groups were extracted from the Greenwich Observatory Catalogue at Internet *http://solarscience.msfc.nasa.gov /greenwch.shtml*. Thus, all the quantities studied in this paper relate to the solar latitudes within $\pm 40^\circ$ only.

We use our original database of the CGLB measurements. For a description of the data and its uniformity see more in Sýkora (1971), Storini and Sýkora (1997), Sýkora and Rybák (2005). The CGLB is measured daily in so called absolute coronal units (a.c.u.). The measurements are performed along the solar limb with 5° a step in the position angle and refered to the height of $60''$ above the limb. Thus any synoptic map based on these measurements has the step of $\sim 13^\circ$ and 5° in the solar longitude and latitude, respectively. Based on the 784 synoptic maps a movie was produced showing a long-term cyclic evolution of coronal brightness (Badalyan *et al.*, 2004; 2005; *http://helios.izmiran.rssi.ru/hellab/ Badalyan/green/*).

The coronal magnetic field was calculated by Badalyan and Obridko (2004) using the method described in detail by Hoeksema and Scherrer (1986) and Hoeksema (1991). The calculations of the magnetic field strength were made under the assumption of a potential approximation from the photospheric measurements of the Wilcox Solar Obs. (*http://wso.stanford.edu/synopticl.html*). A software allowing to derive all the magnetic field components from the photosphere to the source surface level was used (Kharshiladze and Ivanov, 1994). The synoptic charts of the magnetic field strength can be calculated for an arbitrary moment considered to be the central meridian position. As known the original

WSO measurements and, therefore, also the calculated magnetic field data are limited by $\pm 70^{\circ}$ of solar latitude. In our calculations the summarization over 10 harmonics was applied and a polar correction was introduced, considering rather low reliability of the magnetic field measurements close to the solar poles (Obridko and Shelting, 1999). For the purposes of our present paper, we have calculated the coronal magnetic field strength B at the height of $1.1 R_{\odot}$ (approximately corresponding to the height of $60''$ above the limb to which the CGLB measurements are related).

In the performed here analysis, the synoptic charts plotted from the data averaged over six successive Carrington rotations, subsequently shifted by one rotation, were used. Such a procedure permits comprehensive investigation of the large-scale and long-term variations in the mutual relations of the CGLB with both the magnetic field and the areas of sunspot groups. At such a relatively large spatial and time averaging of data an application of the potential approximation and restriction of the number of harmonics during calculations is quite reasonable for description of any large-scale slowly variable solar parameters.

3. Comparison of the coronal green line brightness with the coronal magnetic field strength and with position and size of the sunspot groups

Our study is performed for cycles 21, 22, and 23 (1977-2001). The mean coordinates of the sunspot groups, observed for more than three days during their passage on the Sun's disk were determined. Then, positions of these sunspot groups were plotted onto the corresponding CGLB and magnetic field strength maps (altogether, 329 pairs of maps were at our disposal). Examples of such pairs of maps are demonstrated in Figs. 1-3, where the CGLB maps (upper panels and left legends below) in a.c.u. and the magnetic field strength maps (lower panels and right legends) calculated for the distance of 1.1 $R_{\odot}$ and expressed in μT, are given. Identical sunspot groups denoted by the dark circles corresponding to the size of groups are depicted into each of the map couples. As already mentioned, each of the synoptic maps represents an average of the data from six individual Carrington rotations and the plotted sunspot groups refer to the same time intervals. The maps demonstrated in this paper relate to the 22nd solar activity cycle (examples of the a similar pair of maps, but related to the 21st cycle are shown in Bludova and Badalyan, 2006).

In Fig. 1 the pair of synoptic charts related to the ascending branch (Carrington rotations 1798-1803) of the 22nd solar cycle are exemplified. The entire range of values of the studied parameters in this (and in all the other pairs of maps, including those in Figs. 2 and 3) is divided into sub-ranges, when the darker shading corresponds to the larger values of the CGLB and magnetic field strength. The corresponding levels of the both parameters are clearly separated by the outlined isolines. In the upper map the step between the adjacent iso-

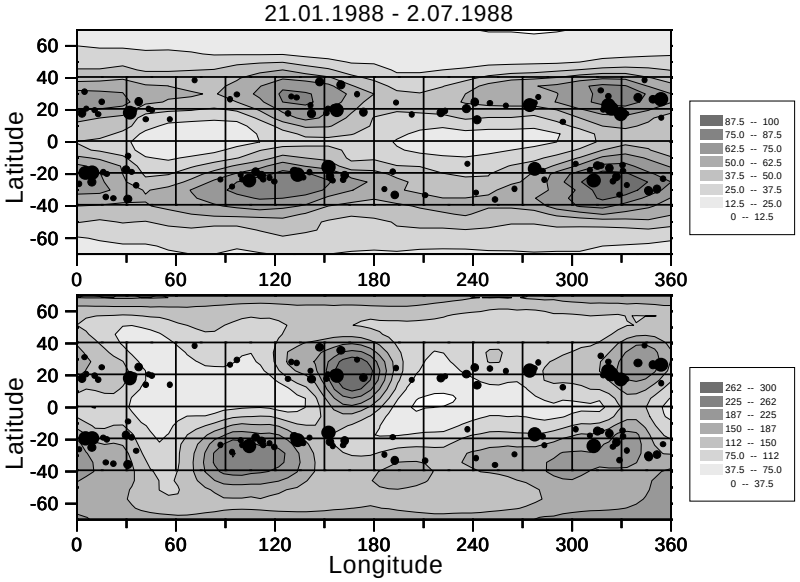

Figure 1. Distributions of the coronal green line brightness (CGLB) (upper chart), the magnetic field strength in the inner corona (lower chart) and positions of the sunspot groups (black circles) observed at the corresponding part of the ascending branch in the 22nd solar activity cycle. The size of the black circles corresponds to the magnitude of the sunspot groups. The CGLB scale is in so called absolute coronal units (a.c.u.) and the magnetic field strength is in micro-Tesla (μT).

lines represents difference of 12.5 a.c.u., whereas in the lower map it is 37.5 μT. During the shown period the magnetic field strength is relatively high, but the CGLB does not reach the highest values. Comparing two maps in Fig. 1, one can notice quite a good mutual spatial correspondence of the field strength and CGLB. Not so well manifested seems to be the correspondence of the sunspot activity with the both mentioned parameters. Namely, in the upper map the largest sunspots do not trace convincingly the most active CGLB regions.

The charts in Fig. 2 refer to the maximum of solar activity (Carrington rotations 1822-1827). The CGLB and, particularly, the magnetic field strength are enhanced during this period in comparison with those in Fig. 1. Gradations of the isolines are now 16 a.c.u. and 55 μT, respectively. Correspondence between the CGLB and the magnetic field strength is rather low (practically absent), especially, in the northern hemisphere. At the same time, agreement of the enhanced CGLB regions with positions and magnitude of sunspots seems to be distinctly better.

Finally, the charts in Fig. 3 belong to the period of the descending branch in the solar cycle (Carrington rotations 1890-1895). Both the CGLB and the

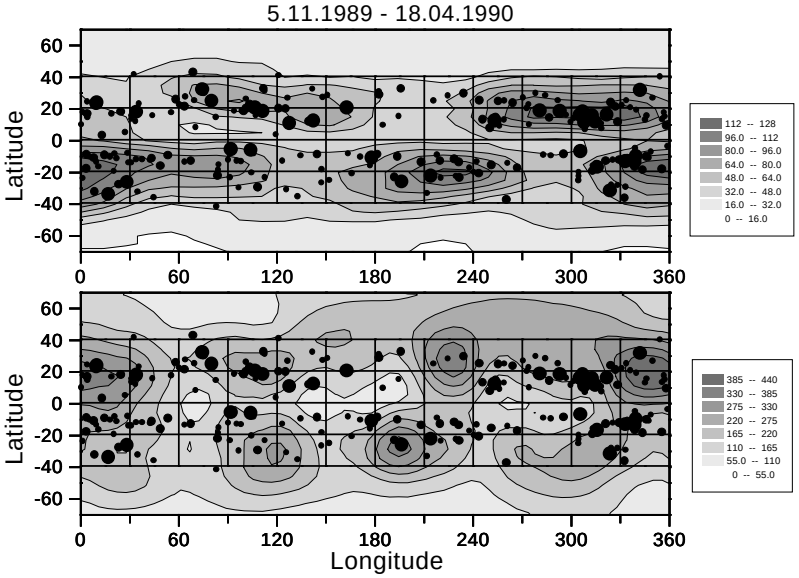

Figure 2. The same as in Fig.1, but now for the period close to maximum of the 22nd cycle.

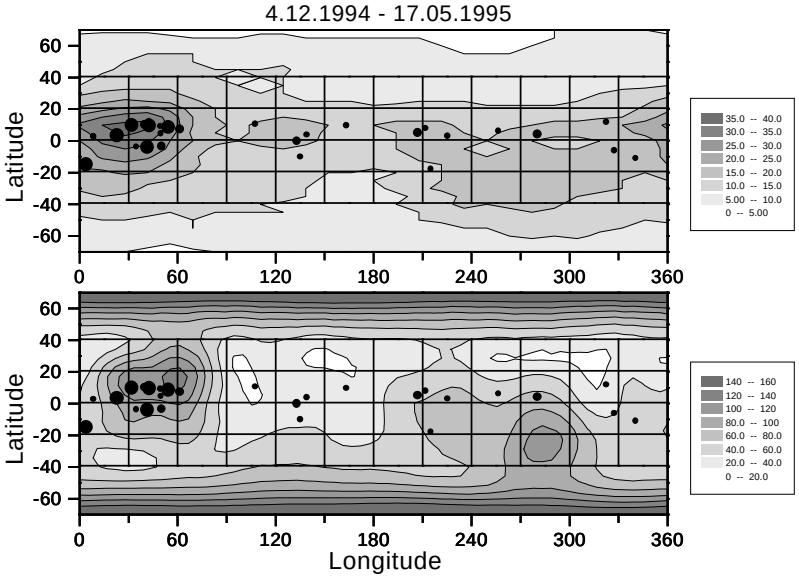

Figure 3. The same as in Fig.1, but now for the final part of the 22nd cycle.

magnetic field strength substantially decrease in comparison with the two above periods (Figs. 1 and 2). Now, gradation of the isolines is only 5 a.c.u. and 20 μT in the upper and lower panels, respectively. Comparison of two charts in Fig. 3 again reveals quite a good correspondence of active regions on both the maps. The largest sunspot groups well lie on the brightest CGLB regions.

A correlation analysis has been performed to estimate quantitatively the above impressions based on the paired comparisons of maps. For this purpose, the mean values of the CGLB, the magnetic field strength, and the summary sunspot areas S_{sum} were determined for the rectangles (the "cells", in the next) 30° in longitude and 20° in latitude on each of the 329 pairs of maps within ±40° of solar latitude. Examples of the resulting grids of 48 cells on each individual map are drawn in Figs. 1-3, as well. Unlike Bludova and Badalyan (2006) a somewhat different index characterizing the summary areas of sunspot groups has been used in this paper. While in Bludova and Badalyan (2006) the areas of all sunspot groups were summed up at the maximum phase of their evolution, in the present work a total sum of all the measured areas of each sunspot group during all days of their observation on the solar disk were considered as S_{sum}. This means that if a sunspot group was observed during, e.g., 10 days, then, S_{sum} includes all 10 values of the area. This kind of an index better reflex the lifetime of the group, i.e., it better characterizes a total "power" of the group. We consider this index to be more adequate for comparisons with the CGLB quantities.

Subsequently, using the sets of 48 values obtained for two maps of each corresponding chart pair the correlation coefficients (CC) between the CGLB and the magnetic field strength and between the CGLB and the areas of sunspot groups, were calculated. In the process of the CC calculations only those cells were considered inside which some sunspot groups were recorded (i.e., the "empty" cells were not taken into account). Thus, as an example, Table 1 provides correlation coefficients k_1 between the CGLB and the magnetic field strength and the correlation coefficients k_2 between the CGLB and the sunspots, all as derived from the synoptic charts in Figs. 1-3. These CC values confirm numerically the conclusions mentioned above from simple visual comparisons of the charts and the sunspot groups on them.

Table 1. Correlation coefficients k_1 between the CGLB and the magnetic field strength and k_2 between the CGLB and the sunspots.

Rotations	Time periods	k_1	k_2
1798-1803	21.01.1988–2.07.1988	0.67	0.20
1822-1827	5.11.1981–18.04.1990	0.14	0.44
1890-1895	4.12.1994–17.05.1995	0.91	0.76

Calculations of the correlation coefficients k_{sum}, performed in this work on the basis of the summarized areas of sunspot groups, do not differ practically from the coefficients k_{max} obtained in (Bludova and Badalyan, 2006) by summarizing the maximum areas of the sunspot groups only. Mutual correlation of the k_{sum} and k_{max} coefficients reaches 0.969 ± 0.003 if considering the whole set of 329 charts. To demonstrate a close relationship of the both coefficients, the $k_{max} - k_{sum}$ are presented in Fig. 4. Noticeably, a weak prevalence of the k_{max} is visible, but still, it does not exceed 0.025 on average.

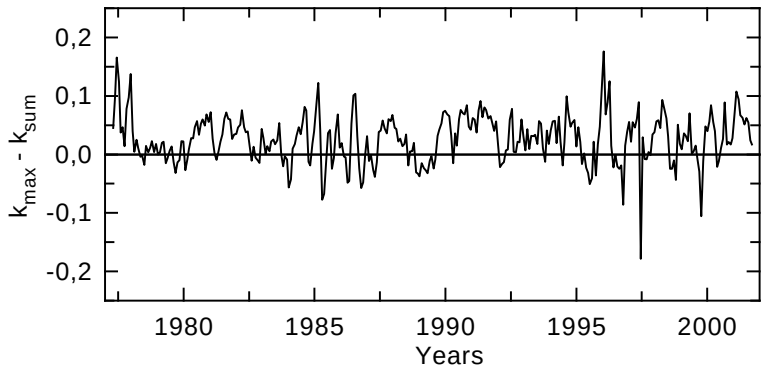

Figure 4. The time course of differences between the correlation coefficients k_{max} by Bludova and Badalyan (2006) and the k_{sum} coefficients computed by a modified approach to the initial data in this work.

Similarity between the correlation coefficients k_{max} by Bludova and Badalyan (2006) and k_{sum} of this paper, stemming from Fig. 4, probably results from the fact that the both indices S_{max} and S_{sum} are comparable in magnitude for each sunspot group in the 1977-2001 period. A close relation of two mentioned indices is evident also from Fig. 5 providing the correlation coefficient 0.949 ± 0.001 (only slightly lower than that for the above "correlation of correlation coefficients"). The x-coefficient in the regression equation (inserted in Fig. 5) apparently represents the lifetime of a typical sunspot group - it amounts to 8 days.

The course of the k_{sum} correlation coefficients is drawn in the upper panel of Fig. 6 by the thin full and dotted lines, representing correlations of the CGLB with the areas of sunspot groups and with the coronal magnetic field strength, respectively. The thick lines in Fig. 6 represent better the long-term variations of the correlation coefficients in question. These curves were obtained by a "filtration" method. In this method the series of n values of the corresponding correlation coefficient (in our case $n = 329$) was expanded into the Fourier series of $n/2$ harmonics and, then, a backward summation (convolution) was performed over a smaller number of harmonics. The convolution of the $n/2$ harmonics describes almost exactly the original distribution and, at the same

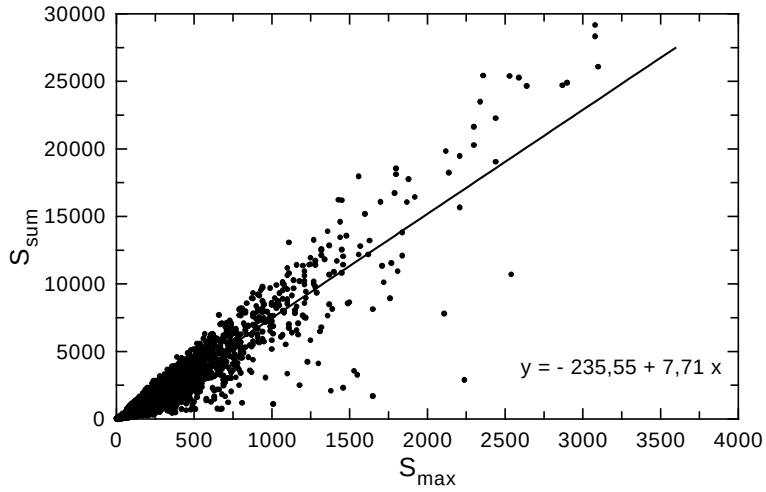

Figure 5. Comparison of the sunspot activity index S_{max} by Bludova and Badalyan (2006) with the S_{sum} index in this paper. The coefficient with x in the regression equation (as written inside the figure) represents a mean lifetime of sunspot groups.

time, such convolution over a smaller number of harmonics permits to cut off the high-frequency harmonics. In the case under discussion, the convolution was performed over the first 5 harmonics, i.e., the harmonics with a period of less than 5 years were cut off. In the lower panel of Fig. 6 the course of Wolf numbers is shown for 21-23 solar cycles. One can see that the correlation coefficients of the CGLB with the magnetic field strength and the summarized areas of sunspot groups behave differently during a solar cycle (see more below).

The correlation coefficients as a function of the cycle phase Φ is demonstrated in Fig. 7. Here, the cycle phase Φ was calculated according to Mitchell's (1929) definition as $\Phi = (\tau - m)/(|M - m|)$, where τ is the running moment of time and M and m are the moments of the nearby maximum and minimum in a given 11-year cycle, respectively. According to this definition the $\Phi = 0$ is identical with the cycle minimum. At the ascending branch of any solar cycle the phases are positive and at the descending branch they are negative. The values $\Phi = \pm 1$ correspond to maxima of the adjacent cycles. Each point in the graph represents the mean value from the correlation coefficients found within the 0.1 interval in the cycle phase. At each of the points the standard deviation is drawn. The open circles and the upper curve relate to correlation of the CGLB with the magnetic field strength, whereas the solid circles and the lower curve demonstrate the course of the CGLB correlation with the areas of sunspot groups. Approximating curves clearly show different behavior of the two correlation coefficients with the solar cycle phase.

We should comment on two points (solid circles) situated close to $\Phi = 0$

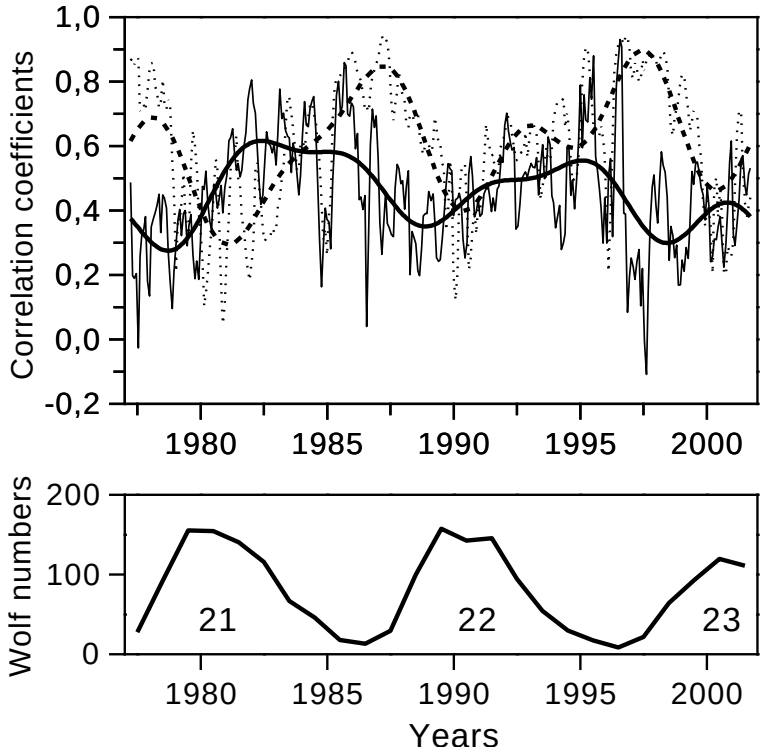

Figure 6. Upper panel demonstrates time courses of the correlation coefficients of the CGLB with the magnetic field strength in the inner corona (thin dotted line) and with the summary area of sunspots (thin full line) derived from synoptic charts divided into the longitude-latitude cells of 30°x20° in size. The thick lines representing correspondingly the long-term variations of both correlations were derived by a method of filtration (see the text for details). The lower panel in this figure demonstrates the course of the yearly Wolf numbers to make easier orientation as for positions of the individual solar cycle phases.

and related to the lower curve which strongly divert from the drawn sequence of points. This is connected with the fact that the cyclic time course of the correlation coefficient is overlapped by some high-frequency oscillations. Possible existence of such oscillations in the correlation coefficient between the CGLB and magnetic field flux has already been discussed in more detail by Badalyan and Obridko (2004; 2006) and Bludova and Badalyan (2006). It was revealed that the phase of these high-frequency oscillations is almost time-independent. Consequently, in any graph presenting dependence of the correlation coefficients on the cycle phase the high-frequency oscillations related to the subsequent

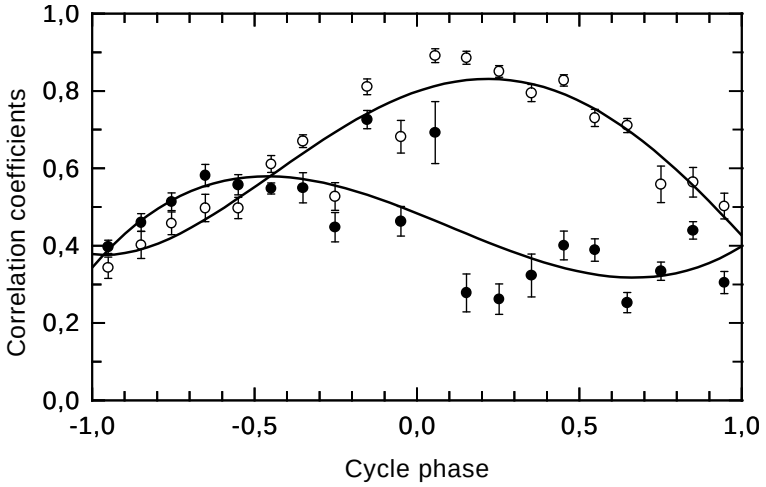

Figure 7. Correlation coefficients as a function of the cycle phase. The CGLB versus magnetic field strength is plotted the by open circles and the CGLB versus areas of the sunspot groups is drawn by filled circles.

cycles overlap mutually (see, e.g., Figure 5 in Bludova and Badalyan (2006), where close to $\Phi = -0.2$ the group of points related to different cycles occupies one and the same region (above the middle curve) in the graph. However, an average of such values, though determined with sufficient accuracy, lies usually well outside of the basic sequence (as, e.g., in Fig. 7 of the present paper).

When calculating the correlation coefficients of the CGLB I with the magnetic field strength B and with the summary areas of sunspot groups S_{sum}, the equations of the linear regressions $I = a_1 + b_1 B$ and $I = a_2 + b_2 S_{sum}$ were solved for each interval of six rotations. By this approach, it is possible to obtain dependence of the regression coefficients a_i and b_i on time t. The $a_1(t)$ function manifests how the CGLB could appear at complete absence of the magnetic field, and $a_2(t)$ function represents the CGLB in the absence of sunspots. Behavior of these functions is shown by thin lines in the upper and lower panels of Fig. 8. The thick lines in both panels of the same figure demonstrate the observed course of $I_{\rm obs}$. In the upper panel, the $I_{\rm obs}$ were averaged within the latitude zone of $\pm 40^\circ$ with successive shifting of the six-rotation interval by one rotation. In the lower panel such averaging was performed considering only those cells (for their definition see above) in which the sunspots were observed. (i.e., the "empty" cells were omitted when calculating $I_{\rm obs}$, similarly as it was done when the correlation coefficients were calculated). It is evident that differences between the thick curves of the upper and lower panels are very small.

The upper panel in Fig. 8 signifies an obvious difference of the thick and thin curves. This difference indicates as if "degree" of the magnetic field influence

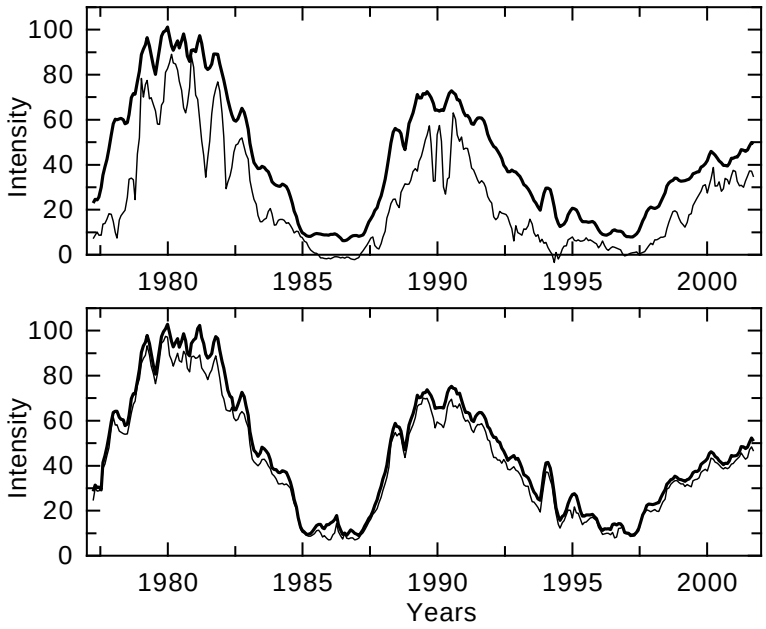

Figure 8. Comparison of the observed CGLB (thick lines on both panels) with the CGLB as if without magnetic field influence (thin line curve on the upper panel and ($a1(t)$ in the text) and as if under absence of sunspots influence (thin line on the lower panel and ($a2(t)$ in the text).

on the level of the CGLB. Then, in the lower panel, the thick and thin curves are almost identical, evoking an apparent "equality" of the CGLB radiation regardless of the presence of sunspots. This implies quite small influence of sunspots on the level of the CGLB.

The differences between the curves in Fig. 8, normalized to $I_{\rm obs}$, are drawn in Fig. 9 in dependence on the cycle phase. The upper and lower curves represent $(a1(t) - I_{\rm obs})/I_{\rm obs}$ and $(a2(t) - I_{\rm obs})/I_{\rm obs}$, respectively. By the points here, the same as in Fig. 7, the averaged values of differences for the step of 0.1 in the cycle phase are given, together with the mean square deviations. Fig. 9 shows that in the zone of $\pm 40^\circ$ during the maximum of a solar cycle only about 25-30% of the CGLB originates under the influence of the large-scale magnetic field, whereas, at the cycle minimum this amount culminates at 85%. The influence of sunspots (i.e., of the local magnetic fields) is substantially lesser. As the lower curve in Fig. 9 shows, it goes to 8-10% only during the maximum and to about 18% in the minimum of a solar cycle (we repeat that these numbers relate to those cells only in which the sunspots really have occurred). Fig. 9 indicates also a certain mutual shifting in the cycle phase at which the maximum "influence" of the

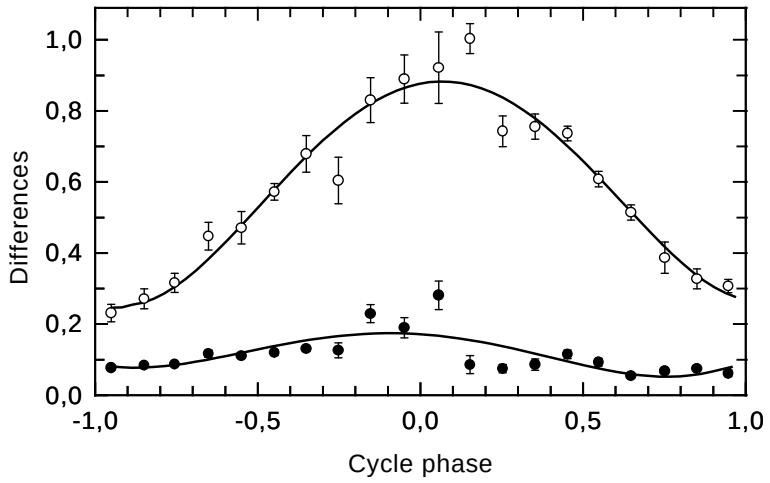

Figure 9. Normalized differences of the pairs of curves from Fig. 8: The cycle dependence of $(a1(t) - I_{\rm obs})/I_{\rm obs}$ (upper curve) and of $(a2(t) - I_{\rm obs})/I_{\rm obs}$ (lower curve) are demonstrated.

magnetic field and of the sunspots appears.

4. On dependence of the calculated correlation coefficients from the longitudinal size of the cells

A testing to reveal a degree of influence of the chosen longitudinal size of cells on the calculated correlation coefficients has been performed. We remind that originally a standard size of 30° in the solar longitude was chosen, responding to an average size of a relatively large active region. In the next, we have made the same calculations, but considering successively the whole set of the longitudinal sizes of cells, going from 15° up to 72°. The original latitude size of the cells 10° was not changed during these additional calculations, i.e., four near-equatorial 10° latitude zones were permanently considered on the northern and southern solar hemispheres.

In Fig. 10 comparisons of the correlation coefficients obtained by using cells of 30° in solar latitude with those derived from the 15° (upper panel) and 60° (lower panel) longitude-size cells. It is evident that time course of the coefficients practically does not depend on dimension of the cells. However, the magnitude of coefficients slightly depends on their size. Note that in the upper panel of Fig. 10 the dotted curve (cells of 15° in longitude) is almost completely situated below the "standard" curve (30° cells), whereas, the lower panel shows almost the whole 60° curve to be displaced above the "standard" 30° curve. By this, Fig. 10 illustrates conclusion that for the smaller than 30° cells, the correlation

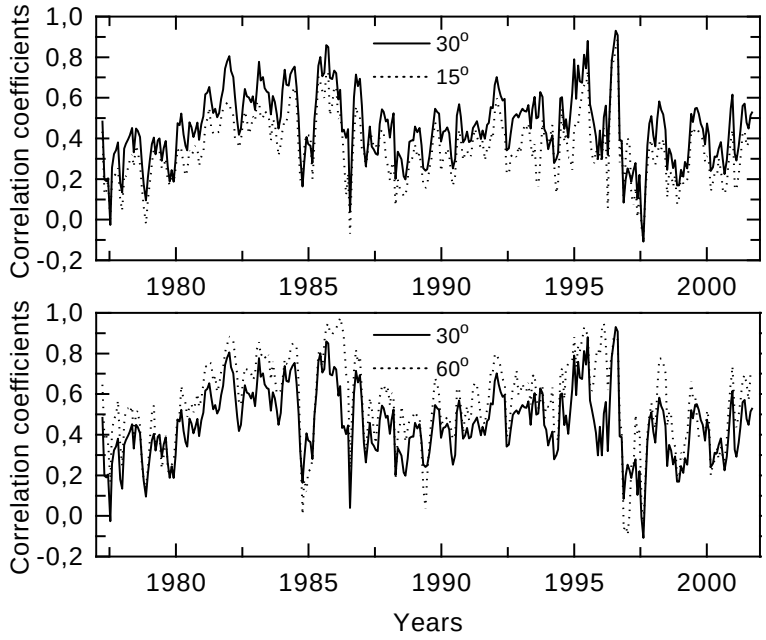

Figure 10. Comparison of the correlation coefficients derived from the cells of 30° in longitude with those derived from the cells of 15° and 60° in longitude (see the upper and lower panels, respectively).

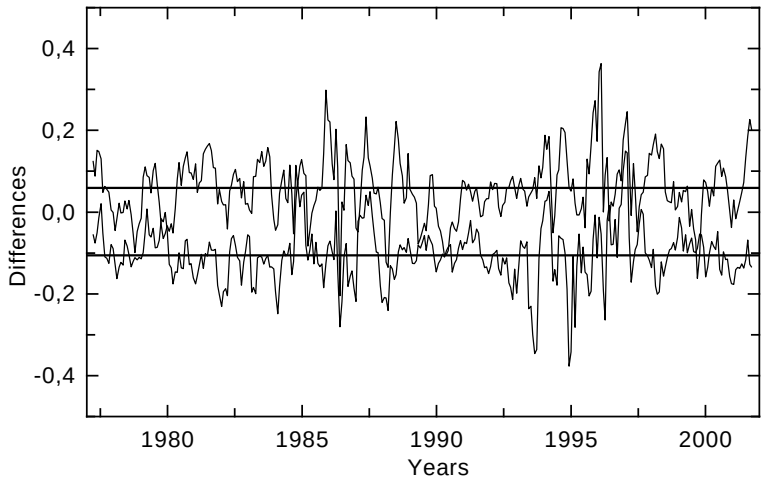

Figure 11. Differences $k_{15} - k_{30}$ and $k_{40} - k_{30}$ of the correlation coefficients may be compared. Two horizontal straight lines represent mean values of these differences.

coefficients are slightly lower and for the larger cells they are somewhat higher than the "standard" ones.

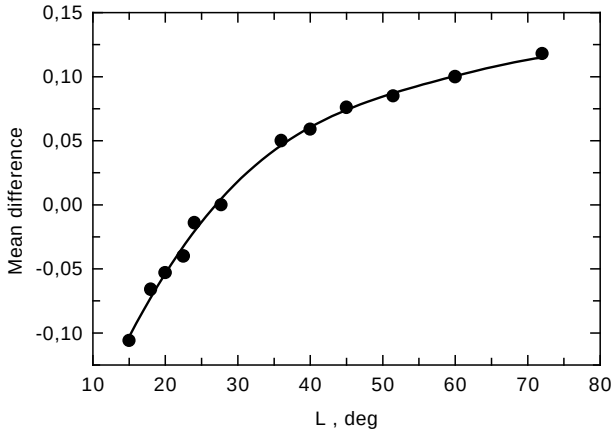

Figure 12. Dependence of the mean differences in the correlation coefficients from the longitudinal size L of the cells.

Differences in coefficients $k_{15} - k_{30}$ and $k_{40} - k_{30}$ are compared in Fig. 11, where two horizontal straight lines represent the mean differences. This figure quantitatively presents two conclusions made above on the basis of visual inspection of Fig. 10. The mean difference of correlation coefficients as a function of the longitudinal cell size L is demonstrated in Fig. 12. It can be well deduced that the correlation coefficients increase only slightly with enlargement of the longitudinal size of cells. This is, most probably, due to correspondingly more extensive integration and averaging of the signal along the line of sight during the CGLB measurements at the solar limb. In any case, it may be concluded that the chosen longitudinal size of cells influences negligibly the correlation coefficients between the CGLB and the areas of sunspot groups..

5. Conclusions

The analysis performed in this work has shown that relations of the CGLB with the magnetic field strength and the areas of the sunspot groups display a cyclic character. At the same time, the corresponding correlation coefficients differently depend on the phase of the 11-year solar cycle. This, in fact means that in dependence on the cycle phase the magnetic fields of various scales differently influence physical conditions in the inner corona, favorable for the coronal green-line emission.

It is worth noticing that during the solar cycle maximum, within the $\pm 40^\circ$ latitude zone only 25-30% of the coronal green-line radiation comes from a synergism of the coronal magnetic field. At the phase of the cycle minimum this portion is considerably higher, going up to 85%. On the other hand, a synergism of the sunspots (representing the local magnetic fields) on the CGLB production is remarkably smaller, representing about 8-10% at the maximum and increasing to 18% at the cycle minimum.

It should be noticed that the commonly accepted scenario about one-way response of the CGLB generation to the increased sunspot formation does not seem generally true. Naturally, the cyclic variations of the Wolf numbers (as well as of the other sunspot activity indices) and the CGLB within the low-latitude zone occur in the phase and almost synchronously. However, as also our analysis proves, the relations between the CGLB and the magnetic fields of different scales are substantially more complicated. It should also be mentioned that the found relationship may be characteristic for the statistical representations only, depicted by the used coronal synoptic charts, the calculated values of the magnetic fields strength and the selected sunspot indices.

Our investigation suggests that a certain common mechanism probably exists governing all the processes in the Sun, including the CGLB, the magnetic field strength and the sunspot formation. This mechanism has a cyclic nature which manifests itself in similar cyclic variations of the total sunspot area, the magnetic field strength and the CGLB. At the same time, Fig. 9 demonstrates these three parameters are not directly related one to another. In other words, a close similarity of the cyclic variations of the sunspot areas (or of the Wolf numbers) and the CGLB does not suggest at all that, e.g., sunspots control the CGLB. There may exist another global agent, probably, associated with a global magnetic field which plays role of such a "governing mechanism".

Acknowledgements. This research was supported by the Russian Foundation for Basic Research (Project No. 05-02-16090) and by the VEGA Grant No. 2/7012/27 of the Slovak Academy of Sciences.

References

Badalyan, O.G., Obridko, V.N.: 2004, *Astron. Zh.* **81**, 746; (English translation *Astronomy Reports* **48**, 678)

Badalyan O.G., Obridko V.N.: 2006, *Solar Phys.* **238**, 271

Badalyan, O.G., Obridko, V.N., Sýkora, J.: 2004, *Astron. Astrophys. Trans.* **23**, 555

Badalyan, O.G., Obridko, V.N., Sýkora J.: 2005, *Astron. Zh.* **82**, 535; (English translation *Astronomy Reports* **49**, 477)

Bludova N.G.: 2005, *Astron. Astrophys. Trans.* **24**, 39

Bludova N.G., Badalyan, O.G.: 2006, *Pisma v Astron. Zh.* **32**, 777; (English translation *Astron. Lett.* **32**, 698)

Guhathakurta, M., Fisher, R.R., Altrock, R.C.: 1993, *Astrophys. J., Lett.* **414**, L145

Guhathakurta, M., Fisher, R., Strong, K.: 1996, *Astrophys. J., Lett.* **471**, L69

Fisher, R., Musman, S.: 1975, *Astrophys. J.* **195**, 801
Hoeksema, J.T.: 1991, *Solar Magnetic Fields - 1985 through 1990*, Report of Center for Space Science and Astronomy, ASTRO-91-01, Stanford University
Hoeksema, J.T., Scherrer, P.H.: 1986, *The Solar Magnetic Field – 1976 through 1985*, WDCA Report UAG-94, NGDC, Boulder
Kharshiladze, A.P., Ivanov, K.G.: 1994, *Geomagnetizm i Aeronomia* **34 (4)**, 22 (in Russian)
Letfus, V., Kulčár, L., Sýkora, J.: 1980, in *Solar and Interplanetary Dynamics*, eds.: M. Dryer and E. Tandberg-Hanssen, Reidel, Dordrecht, 49
Mitchell, S.A.: 1929, *Handbuch der Astrophysik* **4**, 231
Obridko, V.N., Shelting, B.D.: 1999, *Solar Phys.* **184**, 187
Rušin, V., Rybanský, M.: 2002, *Solar Phys.* **207**, 47
Storini, M., Sýkora, J.: 1997, *Nuovo Cimento* **20C**, 923
Sýkora, J.: 1971, *Bull. Astron. Inst. Czechosl.* **22**, 12
Sýkora, J.: 1992, *Solar Phys.* **140**, 379
Sýkora, J., Rybák, J.: 2005, *Adv. Space Res.* **35**, 393
Wang, Y.-M., Sheeley, N.R. Jr., Hawley, S.H., Kraemer, J.R., Brueckner, G.E., Howard, R.A., Korendyke, C.M., Michels, D.J., Moulton, N.E., Socker, D.G.: 1997, *Astrophys. J.* **485**, 419
Zhang M., Zhang H.Q., Ai G.X., Wang H.N.: 1999, *Solar Phys.* **190**, 79